# Combination therapy with dendritic cell vaccine and programmed death ligand 1 immune checkpoint inhibitor for hepatocellular carcinoma in an orthotopic mouse model

**Chiao-Fang Teng, Ting Wang, Tzu-Hua Wu, Jia-Hui Lin, Fu-Ying Shih, Woei-Cherng Shyu and Long-Bin Jeng** (ID)

## Abstract

**Background:** Hepatocellular carcinoma (HCC) is among the most common and lethal human cancers worldwide. Despite remarkable advances in treatment, high mortality in HCC patients remains a big challenge. To develop novel therapeutic strategies for HCC is thus urgently needed to improve patient survival. Dendritic cells (DC)-based vaccines can induce tumor-specific immunity and have emerged as a promising approach for treating HCC patients; however, its effectiveness needs to be improved. Recently, blockade of programmed death ligand 1 (PD-L1) immune checkpoint pathway has been shown to enhance anti-tumor immune responses and exhibited great potential in HCC therapy.

**Methods:** In this study, we generated DC vaccine by pulsing the C57BL/6J mouse bone marrow-derived DC with mouse hepatoma Hep-55.1C cell lysate. We developed a therapeutic strategy combining DC vaccine and PD-L1 inhibitor for HCC and evaluated its efficacy in an orthotopic HCC mouse model in which Hep-55.1C cells were directly injected into left liver lobe of C57BL/6J mouse.

**Results:** Compared with a control group of mice, groups of mice treated with DC vaccine or PD-L1 inhibitor had significantly improved overall survival, reduced tumor volume, and increased tumor cell apoptosis. Remarkably, combination treatment with DC vaccine and PD-L1 inhibitor led to considerably longer overall survival, smaller tumor volume, and higher tumor cell apoptosis of mice than either treatment alone in a dose-dependent manner through inducing a stronger anti-tumor cytotoxic T cell response.

**Conclusion:** Our data suggested that combination therapy with DC vaccine and PD-L1 inhibitor might have great promise as a novel treatment strategy for HCC.

*Keywords:* combination therapy, dendritic cells, hepatocellular carcinoma, immune checkpoint inhibitor, programmed death ligand 1

Received: 30 October 2019; revised manuscript accepted: 3 April 2020.

Correspondence to:
**Chiao-Fang Teng**
Graduate Institute of Biomedical Sciences, China Medical University, No.91, Hsueh-Shih Rd., Northern Dist., Taichung City 404

Organ Transplantation Center, China Medical University Hospital, Taichung

Research Center for Cancer Biology, China Medical University, Taichung
**chiaofangteng@gmail.com**

**Woei-Cherng Shyu**
Graduate Institute of Biomedical Sciences, China Medical University, No.91, Hsueh-Shih Rd., Northern Dist., Taichung City 404

Department of Occupational Therapy, Asia University, Taichung

Department of Neurology, China Medical University Hospital, Taichung

Translational Medicine Research Center, China Medical University Hospital, Taichung
**shyu9423@gmail.com**

**Long-Bin Jeng**
Organ Transplantation Center, China Medical University Hospital, No.2, Yude Rd., Northern Dist., Taichung City 404
**longbin.cmuh@gmail.com**

**Ting Wang**
**Tzu-Hua Wu**
Organ Transplantation Center, China Medical University Hospital, Taichung

**Jia-Hui Lin**
Graduate Institute of Biomedical Sciences, China Medical University, Taichung

**Fu-Ying Shih**
Program for Biotech Pharmaceutical Industry, School of Pharmacy, China Medical University, Taichung

## Introduction

Hepatocellular carcinoma (HCC) is one of the most frequent human cancers in the world with a high mortality rate, killing 500,000–600,000 people every year.[1–3] Multiple therapeutic approaches have been developed for the treatment of HCC, including surgical resection, liver transplantation, and many nonsurgical therapeutic options, such as radiofrequency ablation, transcatheter arterial chemoembolization, systemic chemotherapy, and targeted therapy.[4–6] However, these treatments exhibit limited survival benefit. HCC displays

high recurrence rates after surgical treatments as well as high resistance to commonly used chemotherapeutic and targeted drugs, leading to poor patient survival.[7–9] Therefore, it is urgently needed to develop a novel, effective, and safe therapeutic strategy for patients with HCC.

Dendritic cells (DC) are the most potent antigen-presenting cells in the human immune system.[10–12] In the immature state, DC are present in the blood and tissues where they sample antigens derived from virally infected, tumorigenic, or foreign cells. Upon uptake of presentable antigens, DC undergo maturation and antigen processing and migrate to lymph nodes where they present antigens to and activate T cells (including the helper and cytotoxic T cells) and produce interleukin 12 (IL-12) to promote T cell proliferation, triggering the antigen-specific immune responses to destroy target cells. Based on these characteristics, DC-based immunotherapy, which stimulates tumor-specific immune responses, has emerged as a promising treatment strategy for HCC.[13,14] Several clinical trials have been carried out to evaluate the efficacy of a DC-based vaccine to treat HCC patients, for example, DC pulsed with whole protein lysates of autologous human tumor cells or human hepatoma cell line HepG2 cells, as well as with peptides derived from known tumor antigens such as $\alpha$-fetoprotein and glypican-3.[15–18] Collectively, these clinical trials demonstrate that a DC-based vaccine is safe and promising in the treatment of HCC patients. However, the overall results of current DC vaccination do not yet generate a significant improvement in clinical outcomes. Therefore, new strategies are needed to increase the effectiveness of DC vaccine-induced immune responses to HCC.

During anti-tumor immune responses, tumor cells may weaken the cytotoxic T cell attack through several regulatory mechanisms, which are called "immune checkpoints," to suppress T cell activation, resulting in immune escape or immune tolerance within the tumor microenvironment.[19–21] Among these regulatory mechanisms, programmed death 1 (PD-1) and programmed death ligand 1 (PD-L1) are the most well-studied receptor and ligand expressed on T cells and tumor cells, respectively; the binding of PD-1 to PD-L1 leads to the inhibition of T cell immune responses.[22–24] As a result, PD-1/PD-L1 monoclonal antibodies, which can block PD-1/PD-L1 from interacting with each other, have been developed as immune checkpoint inhibitors for use in cancer treatment to remove the "brake" on the immune system and restore the ability of T cells to attack tumor cells.[25–27] Many clinical trials are currently ongoing to evaluate the safety and efficacy of PD-1/PD-L1 monoclonal antibodies in the treatment of HCC patients.[28,29] Inspiringly, the preliminary results of the trials show that PD-1/PD-L1 immune checkpoint blockade appears to be a promising immunotherapy against HCC.[30]

For these reasons, in this study, we aim to develop a therapeutic strategy combining DC-based vaccine and PD-L1 immune checkpoint inhibitor for the treatment of HCC and evaluate its efficacy in an orthotopic HCC mouse model.

## Methods

### Establishment of the orthotopic HCC mouse model

The orthotopic HCC mouse model was established as described.[31] Briefly, 8-week-old immune-competent C57BL/6J male mice (median weight, 25 g; range, 23–28) were purchased from National Laboratory Animal Center (Taipei, Taiwan) and were anesthetized with isoflurane and subjected to midline laparotomy. $2 \times 10^6$ of the mouse hepatoma Hep-55.1C cells, which were purchased from Cell Lines Service (Eppelheim, Germany) and maintained in DMEM medium (Invitrogen, Carlsbad, CA, USA) supplemented with 10% fetal bovine serum (FBS; Gibco, Grand Island, NY, USA) and $1 \times$ penicillin/streptomycin (P/S; Invitrogen), were directly injected into the left liver lobe of mice. Following hemostasis, the abdomen was closed in two layers. After surgery, the overall survival of mice was followed and the mice tumor burden was recorded when mice died. All animals were housed in individually ventilated cages containing corncob bedding in the animal room of the China Medical University (Taichung, Taiwan) at a constant temperature of $22 \pm 1°C$ and a fixed 12-hour light-dark cycle under specific pathogen-free conditions. All animal experiments were performed under the approval of the Institutional Animal Care and Use Committee of the China Medical University (Approval No: 2016-360 and 2017-330) in accordance with relevant guidelines and regulations.

## Measurement of tumor volume and histopathology

When mice died, the body weight was recorded and the liver was isolated for imaging. The tumor volume was calculated according to the equation $V = 1/2 (L \times W^2)$, where V is the tumor volume, L the length, and W the width, and was expressed as a ratio of tumor volume to body weight for comparison among mice. To evaluate tumor histopathology, the formalin-fixed and paraffin-embedded liver tissues were sectioned into 4 μm thick for hematoxylin and eosin (H&E) staining.

## Generation of the HCC cell lysate-pulsed mature DC (mDC)

In this study, the DC were derived from mouse bone marrow. First, bone marrow was obtained from femurs and tibias of 6-week-old C57BL/6J mice and was digested with collagenase, depleted of red blood cells, passed through a 100-μm filter, and then centrifuged to collect a cell pellet. Next, the cell pellet was resuspended and cultured at a density of $2 \times 10^5$ cells/ml for 6 days in RPMI-1640 medium (Invitrogen) supplemented with 10% FBS (Gibco), $1 \times$ P/S (Invitrogen), $1 \times$ minimum essential medium non-essential amino acids (Invitrogen), 1 mM sodium pyruvate (Invitrogen), 100 ng/ml of human granulocyte macrophage colony-stimulating factor (GM-CSF; Sino Biological Inc., Beijing, China), and 10 ng/ml of interleukin (IL)-4 (Sino Biological Inc.) at 37°C in a humidified 5% $CO_2$ atmosphere. The culture medium and cytokines were refreshed on day 3 of culture. On day 6, the immature DC (iDC) were harvested from the non-adherent and loosely adherent cells in the culture. To generate the mDC, the iDC were next cultured at a density of $1 \times 10^6$ cells/ml in the previous medium with the addition of 1 mg of freeze-thaw Hep-55.1C tumor cell lysate for 30 min, followed by the addition of 50 ng/ml of lipopolysaccharide (LPS; Sigma, Louis, MO, USA) for another day. On day 7, all the cultured cells were collected as the mDC and used as the DC vaccine.

## Flow cytometry analysis of DC phenotypes

The iDC and mDC were washed with phosphate-buffered saline (PBS), aliquoted into fractions ($5 \times 10^5$ cells/100 μl), and then stained for 30 min in the dark at room temperature with a final concentration of 5 μg/ml of the following antibodies purchased from BD Biosciences (San Jose, CA, USA): fluorescein isothiocyanate (FITC)-conjugated anti-CD11c (553801), FITC-conjugated anti-CD40 (553790), FITC-conjugated anti-CD80 (553768), and FITC-conjugated anti-CD86 (553691). As for the negative or no-antibody control, the cells were also stained with corresponding FITC-conjugated isotype-matched control antibodies or remained unstained. After staining, the cells were washed with PBS twice and analyzed by a BD LSRII flow cytometer (BD Biosciences). Data analysis was performed using FlowJo software (Tree Star, San Carlos, CA, USA). The cells positive for FITC-CD11c were considered as DC that had successfully differentiated from bone marrow cells. The cells positive for FITC-CD40, FITC-CD80, and FITC-CD86 were considered as DC that had undergone successful maturation. For concurrent analysis of these molecules, the mDC were stained with phycoerythrin-indotricarbocyanine (PE-Cy7)-conjugated anti-CD11c (558079; BD Biosciences), together with the FITC-conjugated anti-CD40, FITC-conjugated anti-CD80, and FITC-conjugated anti-CD86, respectively.

## FITC-conjugated dextran (FITC-dextran) uptake assay

The iDC and mDC were either left untreated or incubated with 1 mg/ml of FITC-dextran (MW4000; Sigma) at a density of $1 \times 10^6$ cells/ml in RPMI-1640 medium (Invitrogen) supplemented with 10% FBS (Gibco) and $1 \times$ P/S (Invitrogen) for 30 min in the dark at 37°C to allow for phagocytosis or on ice to stop phagocytosis as the negative control. After incubation, the cells were washed with ice-cold PBS twice and analyzed by a BD LSRII flow cytometer (BD Biosciences). Data analysis was carried out using FlowJo software (Tree Star). The FITC-positive cells were considered as cells that had successfully phagocytosed dextran. The experiments were performed three times independently.

## Detection of IL-12 production

The iDC and mDC were cultured at a density of $1 \times 10^6$ cells/ml in RPMI-1640 medium (Invitrogen) supplemented with 10% FBS (Gibco) and $1 \times$ P/S (Invitrogen). After 1 day in culture, the supernatants were collected and measured by an enzyme-linked immunosorbent assay (ELISA) for IL-12 p70 using the Mouse IL-12 (p70) ELISA Set (BD Biosciences) following the manufacturer's instructions. The experiments were performed in triplicate three times independently.

### T cell proliferation assay

To isolate T cells, spleen cells were obtained from 6-week-old C57BL/6J mice using the same procedures described previously as for bone marrow cells, followed by separation by a density gradient centrifugation with the Ficoll-Paque PLUS (density 1.077 g/ml; GE Healthcare, Uppsala, Sweden). The co-culture of DC (iDC or mDC) and T cells was carried out by placing cell culture inserts (pore size 0.4 µm; Falcon, Oxnard, CA, USA) onto each well of a 24-well plate, followed by seeding DC and T cells into the wells and inserts at a density of $2 \times 10^5$ cells/well and $1 \times 10^5$ cells/insert, respectively, in RPMI-1640 medium (Invitrogen) supplemented with 10% FBS (Gibco) and $1 \times$ P/S (Invitrogen). After 3 and 6 days in culture, T cells were collected from each insert and live cells were counted immediately by a Countess Automated Cell Counter (Invitrogen). The experiments were performed in triplicate three times independently.

### Cytotoxicity assay

The whole T cell suspensions were prepared from the mouse spleen with the previously mentioned procedures and were co-cultured with or without the mDC at a ratio of 10:1 in the presence or absence of anti-PD-L1 antibody (10 µg/ml). After 3 days in culture, the resulting cells were harvested and then co-cultured with the mouse hepatoma Hep-55.1C cells at a ratio of 100:1 in the presence or absence of anti-PD-L1 antibody (10 µg/ml). After 1 and 2 days in culture, five independent microscopic fields (original magnification, ×20) with the smallest coverage area of Hep-55.1C cells in each group were selected. The total coverage area of Hep-55.1C cells in the five selected fields was quantified by ImageJ software (http://rsb.info.nih.gov/ij) and further calculated as the coverage area of Hep-55.1C cells per field for statistical analysis. For the cytotoxicity assay of cytotoxic T cells, CD8-positive T cells were isolated from the whole T cell suspensions using the mouse CD8$^+$ T Cell Isolation Kit (StemCell Technologies, Vancouver, BC, Canada) following the manufacturer's instructions. The experiments were performed three times independently.

### In vivo *administration of the DC vaccine and PD-L1 inhibitor*

The DC vaccine (mDC) was prepared as described previously. The immune checkpoint inhibitor, the InVivoPlus anti-mouse PD-L1 (BP0101) monoclonal antibody that has rigorous quality control measures, was purchased from Bio X Cell (West Lebanon, NH, USA). On day 7 after tumor cell injection, the orthotopic HCC mice were randomly allocated into one of six treatment groups (six mice/group): the vehicle control, the mDC ($1 \times 10^6$ cells/dose), the anti-PD-L1 (100 µg/dose), the anti-PD-L1 (200 µg/dose), the mDC ($1 \times 10^6$ cells/dose) plus anti-PD-L1 (100 µg/dose), and the mDC ($1 \times 10^6$ cells/dose) plus anti-PD-L1 (200 µg/dose) treatment groups. Also, the difference in mice weight between groups was balanced to minimize the effect of subjective bias. The mDC were subcutaneously injected into the groin area (near lymph node) of mice. The anti-PD-L1 antibody was intraperitoneally injected into mice. Sterile PBS was used as the vehicle control and was injected into the control mice both subcutaneously and intraperitoneally, as well as into the mDC- and anti-PD-L1-treated mice intraperitoneally and subcutaneously, respectively. All treatments were begun on day 7 after tumor cell injection and repeated every other day for three total doses in each group of mice. After treatment, mice were followed until time of death to determine days of survival, followed by measurement of tumor volume, examination of histopathology and cell apoptosis, as well as detection of DC, cytotoxic T cells, and granzyme B-positive cells. No obvious adverse effects were observed in each treatment groups of mice.

### Fluorescent immunohistochemistry (IHC) staining

Fluorescent IHC staining was performed as described.[32] Briefly, the frozen tumor tissues from each treatment group of mice were cut into 4-µm-thick sections. For staining DC, the tissue sections were incubated with the primary antibody FITC-conjugated anti-CD11c (553801; BD Biosciences). For staining cytotoxic T cells, the tissue sections were incubated with the primary antibodies anti-CD3 (ab16669; Abcam, Cambridge, UK) together with anti-CD8 (MA5-13473; Invitrogen), followed by the secondary antibodies Alexa Fluor 488-conjugated goat anti-rabbit IgG (A11008; Invitrogen) together with Alexa Fluor 555-conjugated goat anti-mouse IgG (A-21424; Invitrogen). For staining granzyme B, the tissue sections were incubated with the primary antibody anti-granzyme B (ab4059; Abcam), followed by the secondary antibody Alexa Fluor 488-conjugated goat anti-rabbit IgG

(A11008; Invitrogen). DAPI (4', 6-diamidino-2-phenylindole; Invitrogen) was used to stain the nuclei. Five independent microscopic fields (original magnification, ×40) with the most abundant DC, cytotoxic T cells, or granzyme B-positive cells in tumor tissues of each mouse were selected. The total number of DC, cytotoxic T cells, or granzyme B-positive cells in the five selected fields of each mouse was counted manually and further calculated as the number of DC, cytotoxic T cells, or granzyme B-positive cells per field for statistical analysis.

### In situ *detection of cell apoptosis*
The frozen tumor tissues from each treatment group of mice were cut into 4-μm-thick sections. Cells undergoing apoptosis in the tissue sections were visualized with the terminal deoxynucleotidyl transferase-mediated deoxyuridine triphosphate nick end-labeling (TUNEL) method by using the *in situ* Cell Death Detection Kit, Fluorescein (Roche, Mannheim, Germany) according to the manufacturer's instructions. Nuclei were stained with DAPI (Invitrogen). Five independent microscopic fields (original magnification, ×63) with the most abundant apoptotic cells in tumor tissues of each mouse were selected. The total number of apoptotic cells in the five selected fields of each mouse was counted manually and further calculated as the number of apoptotic cells per field for statistical analysis.

### *Statistical analysis*
The significance of the difference between iDC and mDC in their capacity to uptake dextran, produce IL-12, and stimulate T cell proliferation, as well as between different treatment groups of T cells in their capacity to kill HCC cells was determined by unpaired *t*-test. Data were represented as the mean with the standard error of the mean (SEM) error bar of three independent experiments. The significance of the difference of overall survival time between different treatment groups of mice was determined by Mantel–Cox log-rank test. The significance of the difference between different treatment groups of mice in tumor volume-to-body weight ratio as well as DC, cytotoxic T cell, granzyme B-positive cell, or apoptotic tumor cell number per field was determined by one-way ANOVA followed by Tukey's multiple comparisons test. A *p* value $< 0.05$ was considered significant ($^*p < 0.05$; $^{**}p < 0.01$; $^{***}p < 0.001$).

## Results

### *The orthotopic HCC mice developed tumors in liver and died about 32–38 days after inoculation of tumor cells*
The orthotopic HCC mouse model was established as described in the Methods section (Figure 1a and b). As shown in Figure 1(c), the orthotopic HCC mice (Hep-55.1C mice, $n = 6$) had mean and median survival times of 36 (SEM, 1.00) and 36.5 (range, 32–38) days, respectively, after inoculation of the tumor cells. When mice died, HCC tumors were observed to be orthotopically developed in the liver of all six mice. The ratio [mean $\pm$ SEM (median, range)] of tumor volume to body weight was $215.90 \pm 11.02 \, \text{mm}^3/\text{g}$ (217.3, 178.4–248.5; Figure 1d). Also, the tumor histopathology was evaluated by H&E staining, showing a pattern resembling a poorly differentiated human HCC (Figure 1e).

### *The HCC cell lysate-pulsed mDC displayed appropriate morphology and phenotypes*
The mDC were generated as described in the Methods section (Figure 2a). As shown in Figure 2(b), compared with day 1 of culture, the cells increased gradually and began to form colonies in the suspension on day 3. On day 6 of culture, the cell volume apparently enlarged and the suspended cells began to form dendritic protrusions, a classical dendritic cell morphology, becoming the iDC. Following incubation with Hep-55.1C tumor cell lysate and LPS for another day (day 7), the iDC matured into the mDC with the further elongated dendritic protrusions.

To evaluate the phenotypes of the mDC, flow cytometry was performed to analyze the expression of the DC surface markers, including the identity marker CD11c and the maturation markers CD40, CD80, and CD86. As shown in Figure 2(c) and Figure S1, the iDC expressed high levels of CD11c but low levels of CD40, CD80, and CD86 compared with the mDC expressing high levels of these four molecules individually. Moreover, mDC concurrently expressed high levels of CD11c, CD40, CD80, and CD86 (Figure S2). The data indicated that the mDC we prepared had high purity and maturity.
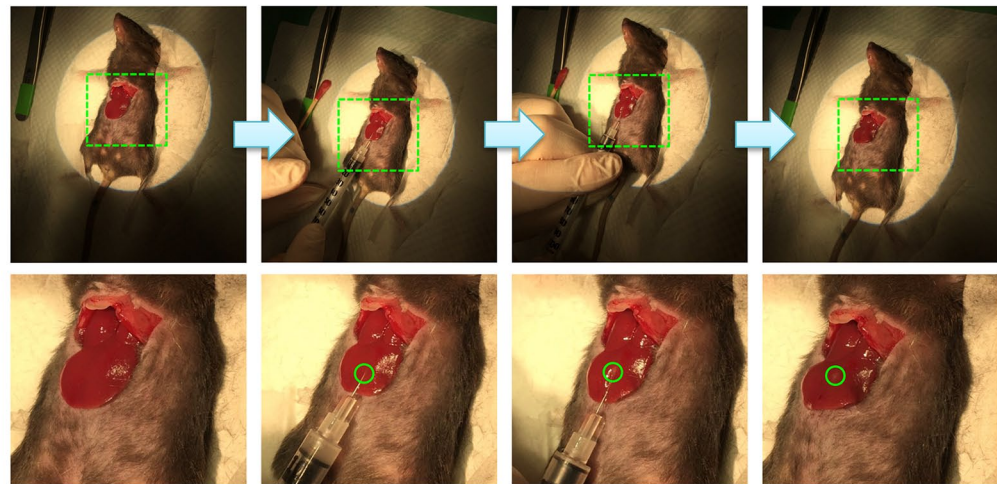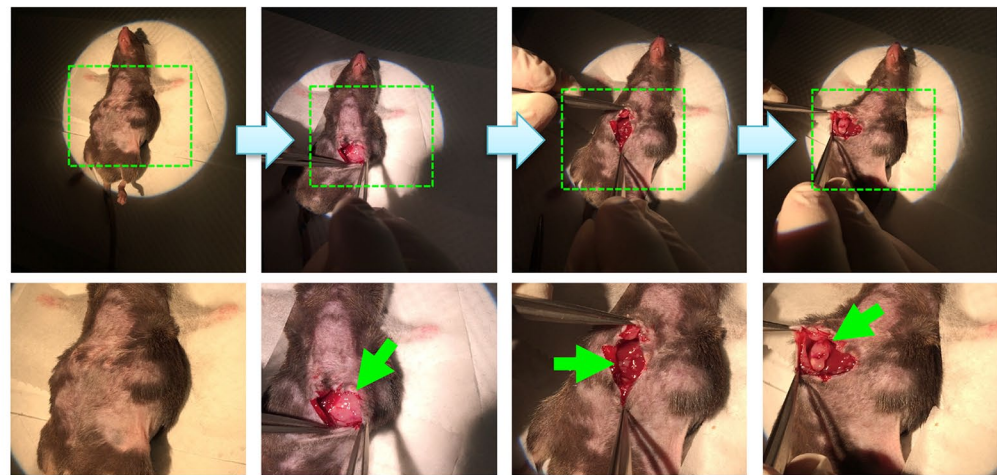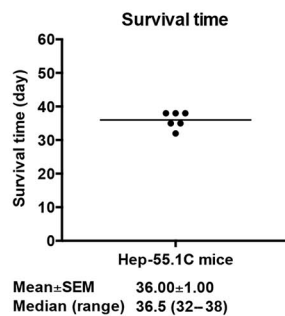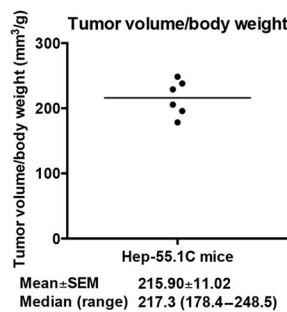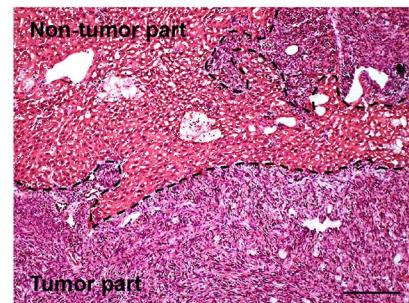
**Figure 1.** Establishment and validation of the orthotopic HCC mouse model. (a) To establish an orthotopic HCC mouse model, the mouse hepatoma Hep-55.1C cells were directly injected into the left liver lobe of the mice undergoing midline laparotomy. The regions indicated with green dashed lines are magnified in the lower panel. The site of cell injection is indicated with green circles. (b) When mice died, tumors were observed to be developed orthotopically in the liver of mice following midline laparotomy. The regions indicated with green dashed lines are magnified in the lower panel. The orthotopic tumors are indicated with green arrows. (c) and (d) Graphs showing the survival time and tumor volume-to-body weight ratio in the orthotopic HCC mice ($n=6$). The horizontal lines represent the mean values. The mean $\pm$ SEM and median (range) values are shown below each graph. (e) Tumor histopathology by H&E staining. Black dashed lines define the regions of tumor and non-tumor parts in the liver tissue. Original magnification, $\times$20. Scale bar, 100 µm.
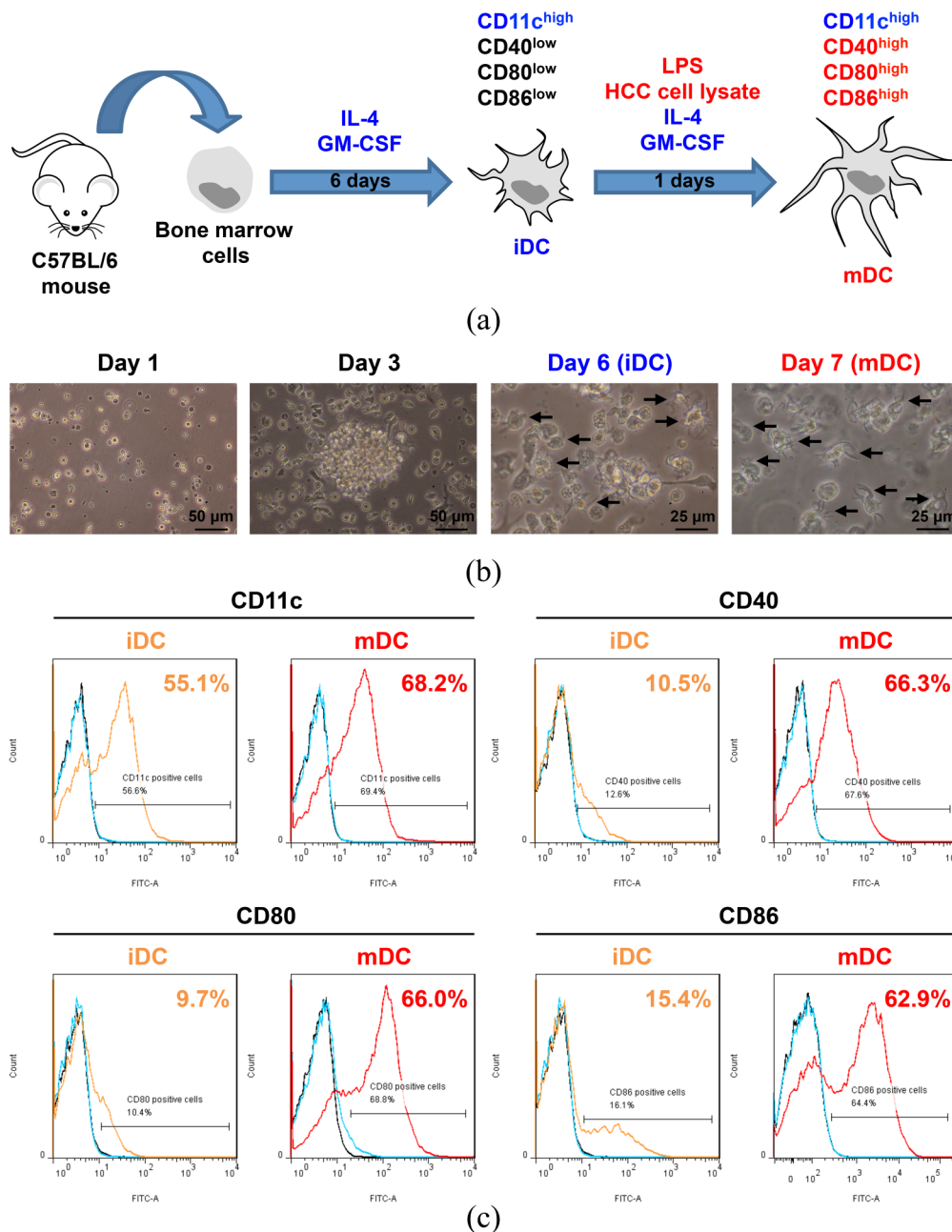HCC, hepatocellular carcinoma; H&E, hematoxylin and eosin.

**Figure 2.** Generation and morphological and phenotypical characterization of the mDC. (a) A schematic diagram illustrating the generation of the mDC from mouse bone marrow. The iDC expressed high levels of CD11c but low levels of CD40, CD80, and CD86 compared with the mDC expressing high levels of these four molecules. (b) Cell morphology examined by inverted phase-contrast microscopy. Black arrows indicate the dendritic protrusions of the suspended cells. Scale bar is shown in the bottom right corner of each image. Original magnification, ×20 (Day 1 and Day 3); ×40 (Day 6 and Day 7). (c) Representative result of flow cytometry analysis of the expression of the DC surface markers, including CD11c, CD40, CD80, and CD86 on the iDC and mDC. For the detection of each marker, the iDC and mDC were either stained with antibodies of each marker (orange and red solid curves, respectively) or isotype-matched control antibodies (cyan solid curves) or remained unstained (black solid curves). The stained cells whose FITC intensity was higher than that of the cells stained with isotype-matched control antibodies were considered as the cells positive for the indicated markers. The number of the cells expressing the indicated markers was calculated as the percentage of all analyzed cells and is shown in the upper right corner of each graph.
DC, dendritic cells; FITC, fluorescein isothiocyanate; HCC, hepatocellular carcinoma; iDC, immature DC; LPS, lipopolysaccharide; mDC, mature DC.
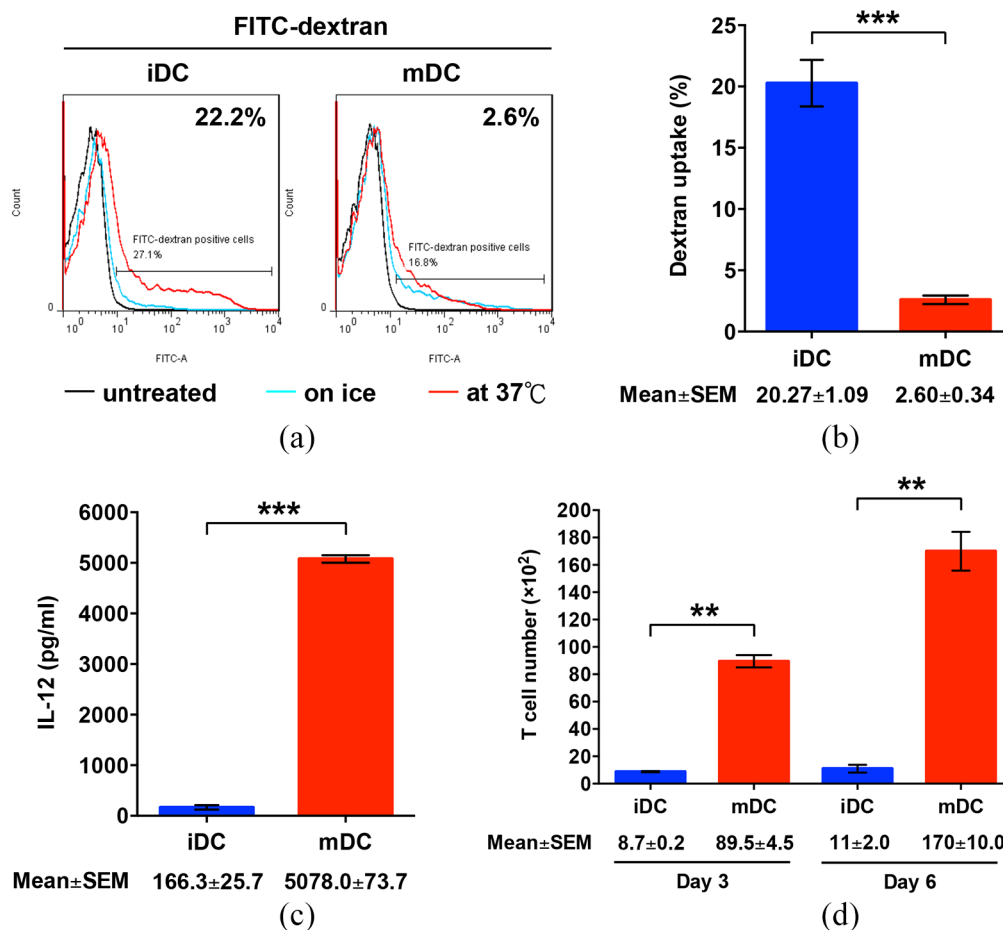
**Figure 3.** Functional characterization of the mDC. (a) For antigen uptake assay, the iDC and mDC were either remained untreated (black solid curves) or incubated with FITC-dextran at 37°C (red solid curves) or on ice (cyan solid curves), followed by flow cytometry analysis. The dextran-treated cells whose FITC intensity at 37°C was higher than that on ice were gated and considered as the cells with the capacity to uptake dextran. Shown are the representative results of three independent experiments. (b) The frequency of the cells positive for FITC-dextran was calculated as the percentage of all analyzed cells. Data represents the mean with SEM error bars of three independent experiments. $^{**}p < 0.01$. (c) IL-12 production by the iDC and mDC. The concentration of IL-12 in the culture supernatants of the iDC and mDC was measured by ELISA and is expressed as the mean with SEM error bars of three independent experiments. $^{***}p < 0.001$. (d) T cell proliferation induced by the iDC and mDC. After co-culture of T cells with the iDC or mDC in cell culture wells, the number of T cells in cell culture inserts was counted on day 3 and day 6 and is shown as the mean with SEM error bars of three independent experiments. $^{**}p < 0.01$.
DC, dendritic cells; ELISA, enzyme-linked immunosorbent assay; FITC, fluorescein isothiocyanate; iDC, immature DC; mDC, mature DC.

### *The mDC exhibited optimal maturation with reduced uptake of antigen and increased capacity to produce IL-12 and promote T cell proliferation*

The DC maturation process is associated with a loss of the capacity of DC to uptake antigens.[12] To compare the antigen uptake capacity between the iDC and mDC, the cells were incubated with FITC-dextran, followed by flow cytometry analysis. As expected, the mDC exhibited significantly decreased levels of FITC-dextran uptake compared with the iDC (mean ± SEM, $2.60 ± 0.34$ *versus* $20.27 ± 1.09$%; $p < 0.001$; Figure 3a and b, and Figure S3).

Mature DC can synthesize high levels of IL-12, which mediates the activation and proliferation of T cells during the engagement between DC
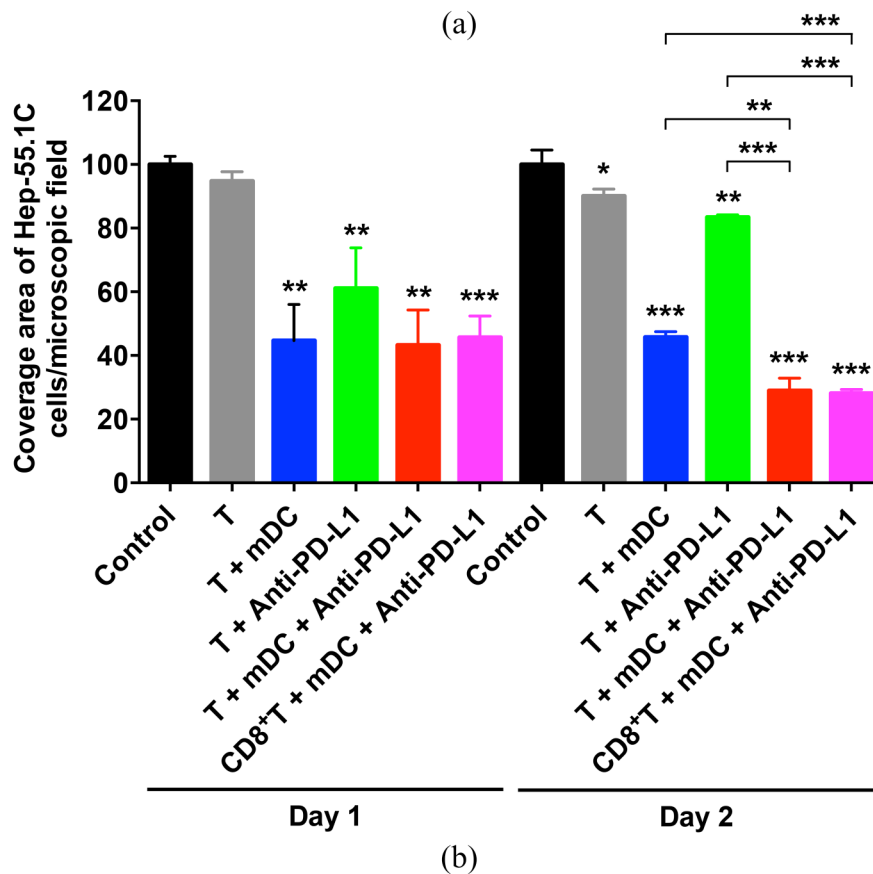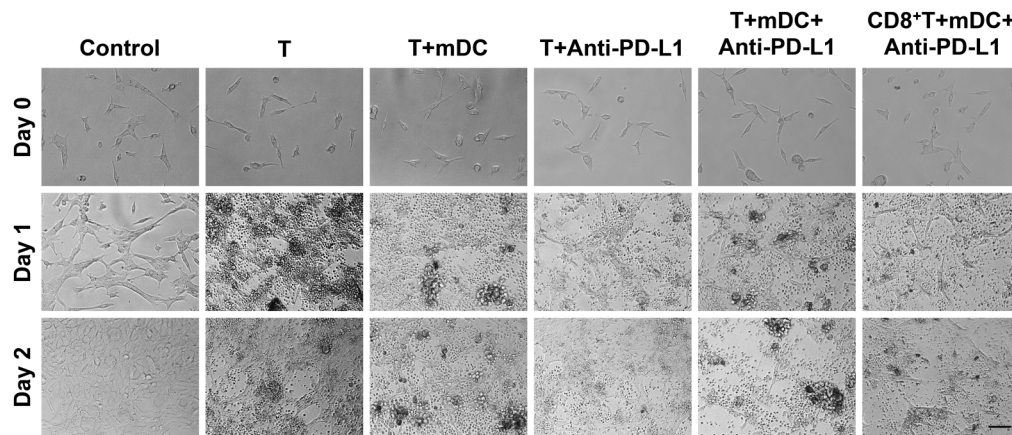
(a)

(b)

**Figure 4.** Verification of cytotoxicity of the mDC either alone or combined with PD-L1 inhibitor treatment against HCC cells. (a) Cytotoxicity assay of the T cells and CD8-positive (CD8^{+}) T cells pre-treated with or without the mDC in the presence or absence of anti-PD-L1 antibody for Hep-55.1C cells on day 1 and 2 after co-culture. Day 0 indicated the day before co-culture of T cells and Hep-55.1C cells. Shown are representative images of each treatment group. Original magnification, $\times$20. Scale bar, 50 $\mu$m. (b) Graph showing the coverage area of Hep-55.1C cells per microscopic field for each treatment group over 2 days of co-culture with T cells. Data represents the mean with SEM error bars of three independent experiments and were relative to the control group (set as 100). The statistical results, shown above each column of treatment group, were compared with the control group on each day. The statistical significance between selected treatment groups was also analyzed.
DC, dendritic cells; HCC, hepatocellular carcinoma; mDC, mature DC.
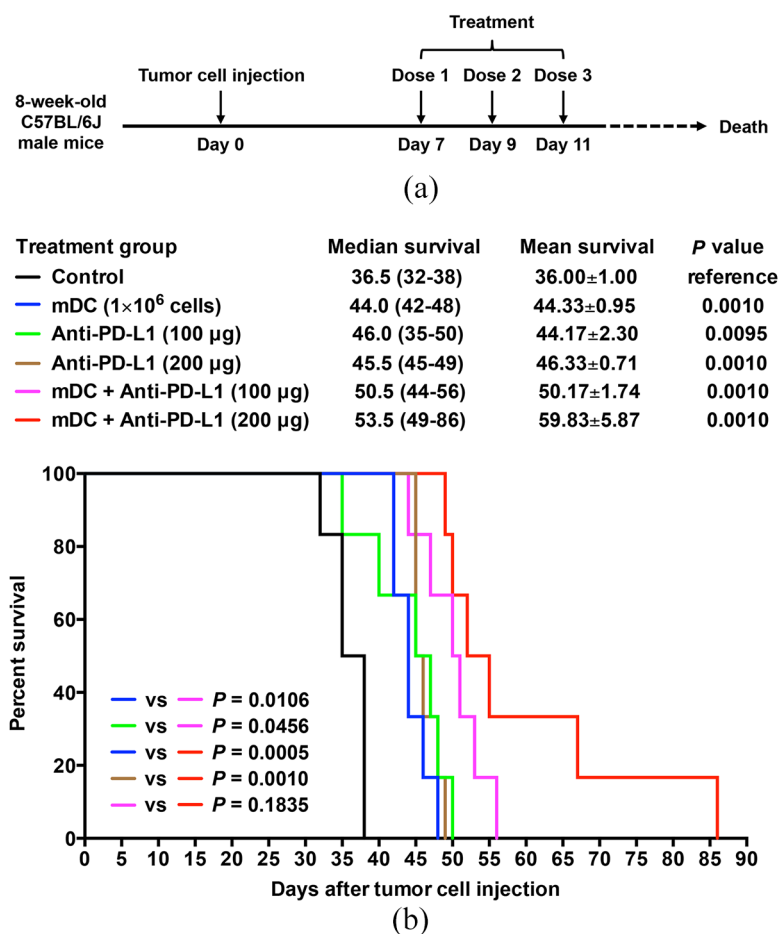[*]$p < 0.05$; [**]$p < 0.01$; [***]$p < 0.001$.

**Figure 5.** Evaluation of survival time of the orthotopic HCC mice after treatment of DC vaccine either alone or combined with PD-L1 inhibitor. (a) Schematic timeline of the mDC and/or anti-PD-L1 treatment schedule in the orthotopic HCC mice. 8-week-old C57BL/6J male mice were injected with Hep-55.1C tumor cells on day 0. Treatment was started on day 7 after tumor cell injection and performed at 1-day intervals for a total of three doses. After treatment, all mice were followed until death to determine survival times. (b) Kaplan–Meier survival curves of the orthotopic HCC mice following treatment with the mDC ($1 \times 10^6$ cells/dose) and/or anti-PD-L1 (100 or 200 μg/dose). The cumulative survival rate was plotted against days after tumor cell injection. The overall survival in each group of mice ($n = 6$) is shown as mean $\pm$ SEM and median (range) in days. The significance of the difference of overall survival between different treatment groups of mice was analyzed and compared with the control group of mice. The significance of the difference of overall survival between single and combined treatment groups was also analyzed and is shown in the lower left corner of the survival plot. A $p$ value $< 0.05$ was considered significant.

DC, dendritic cells; HCC, hepatocellular carcinoma; mDC, mature DC; vs, *versus*.

and T cells.[11] Next, we assessed the capacities of the mDC to secrete IL-12 and stimulate T cell proliferation. As shown in Figure 3(c), IL-12 concentrations were significantly elevated in the culture supernatants of the mDC compared with the iDC (mean $\pm$ SEM, $5078.0 \pm 73.7$ *versus* $166.3 \pm 25.7$ pg/ml; $p < 0.001$). When co-cultured with T cells, the number of live T cells was significantly enhanced by the mDC compared with the iDC on both day 3 (mean $\pm$ SEM, $89.5 \pm 4.5 \times 10^2$ *versus* $8.7 \pm 0.2 \times 10^2$ cells; $p = 0.0031$) and day 6 (mean $\pm$ SEM, $170 \pm 10.0 \times 10^2$ *versus* $11.0 \pm 2.0 \times 10^2$ cells; $p = 0.0041$; Figure 3d). No difference was observed in the number of dead T cells between these two co-culture groups (data not shown). Collectively, these results indicated that the mDC we prepared had optimal maturation and functions.

## Combination treatment with the mDC and PD-L1 inhibitor induced a stronger cytotoxic T cell-mediated cytotoxicity against HCC cells than either treatment alone

To ascertain the efficacy of the mDC combined with PD-L1 inhibitor in triggering T cell-mediated cytotoxicity against HCC cells, T cells were co-cultured with or without the mDC in the presence or absence of anti-PD-L1 antibody, followed by co-culture with the mouse hepatoma Hep-55.1C cells over 2 days. As shown in Figure 4(a) and (b), T cells pre-treated with the mDC and anti-PD-L1 exhibited a stronger efficacy in killing Hep-55.1C cells than those pre-treated with either the mDC or anti-PD-L1 alone on day 2 after co-culture. To further verify whether cytotoxic T cells mediate the cytotoxicity of the mDC combined with PD-L1 inhibitor against HCC cells, CD8-positive T cells were isolated from the whole T cell suspension for the cytotoxicity assay in Hep-55.1C cells. As shown in Figure 4(a) and (b), CD8-positive T cells pre-treated with the mDC and anti-PD-L1 could induce a similar level of cytotoxicity against Hep-55.1C cells to the whole T cell suspension pre-treated with the mDC and anti-PD-L1, suggesting that cytotoxic T cells was the major subtype of T cells contributing to the cytotoxicity of the mDC combined with PD-L1 inhibitor against HCC cells.

## Combination treatment with the DC vaccine and PD-L1 inhibitor led to longer overall survival and smaller tumor volume than either treatment alone in the orthotopic HCC mice

To evaluate the efficacy of the DC vaccine combined with PD-L1 inhibitor for the treatment of HCC, the orthotopic HCC mice (6 mice/group) were administered with three total doses of the mDC ($1 \times 10^6$ cells/dose) and/or anti-PD-L1 antibody (100 or 200 μg/dose) at 1-day intervals and were followed for survival (Figure 5a). As shown in Figure 4(b), the groups of mice treated with the mDC or anti-PD-L1 had significantly improved overall survival compared with the control group of mice [mean ± SEM (median, range); mDC ($1 \times 10^6$ cells/dose), 44.33 ± 0.95 days (44.0, 42–48), $p = 0.0010$; anti-PD-L1 (100 μg/dose), 44.17 ± 2.30 days (46.0, 35–50), $p = 0.0095$; anti-PD-L1 (200 μg/dose), 46.33 ± 0.71 days (45.5, 45–49), $p = 0.0010$]. At 38 days after treatment, all mice in the control group had died, whereas almost all of mice treated with the mDC or anti-PD-L1 (low or high dosage) were still alive and had the longest survival

times of about 48–50 days. However, no significant difference in overall survival was observed between these treatment groups of mice.

Remarkably, combination treatment with the mDC and anti-PD-L1 could considerably further prolong overall survival of mice compared with either treatment alone [mean ± SEM (median, range); mDC + anti-PD-L1 (100 μg/dose), 50.17 ± 1.74 days (50.5, 44–56), $p = 0.0106$ *versus* mDC ($1 \times 10^6$ cells/dose) and 0.0456 *versus* anti-PD-L1 (100 μg/dose); mDC + anti-PD-L1 (200 μg/dose), 59.83 ± 5.87 days (53.5, 49–86), $p = 0.0005$ *versus* mDC ($1 \times 10^6$ cells/dose) and 0.0010 *versus* anti-PD-L1 (200 μg/dose)] (Figure 5b). The longest survival times of mice were extended from about 48 to 50 days by the mDC ($1 \times 10^6$ cells/dose) or anti-PD-L1 (100 or 200 μg/dose) single treatment to 56 days by the mDC + anti-PD-L1 (100 μg/dose), and further to 86 days by the mDC + anti-PD-L1 (200 μg/dose) combined treatment, suggesting that the mDC combined with anti-PD-L1 treatment increased overall survival of mice in a dose-dependent manner, though no significant difference was observed between the mDC + anti-PD-L1 (100 μg/dose) and mDC + anti-PD-L1 (200 μg/dose) treatment ($P = 0.1835$).

Furthermore, the growth of HCC tumors in the liver of each treatment group of mice was also examined when mice died (Figure 6). As shown in Figure 7, in support of the result of mice survival, the groups of mice treated with the mDC or anti-PD-L1 had significantly decreased tumor volume compared with the control group of mice [mean ± SEM (median, range); mDC ($1 \times 10^6$ cells/dose), 128.10 ± 26.97 mm³/g (115.6, 64.7–244.7), $p = 0.0393$; anti-PD-L1 (100 μg/dose), 128.60 ± 26.92 mm³/g (131.6, 48.0–200.2), $p = 0.0411$; anti-PD-L1 (200 μg/dose), 106.80 ± 20.59 mm³/g (101.8, 43.1–195.8), $p = 0.0059$]. However, no significant difference in tumor volume was observed between these treatment groups of mice.

Consistently, combination treatment with the mDC and anti-PD-L1 could lead to considerably smaller tumor volume of mice than either treatment alone [mean ± SEM (median, range); mDC + anti-PD-L1 (100 μg/dose), 67.67 ± 17.47 mm³/g (46.1, 39.1–146.8), $p = 0.2833$ *versus* mDC ($1 \times 10^6$ cells/dose) and 0.2746 *versus* anti-PD-L1 (100 μg/dose); mDC + anti-PD-L1 (200 μg/dose), 14.32 ± 5.83 mm³/g (11.1,
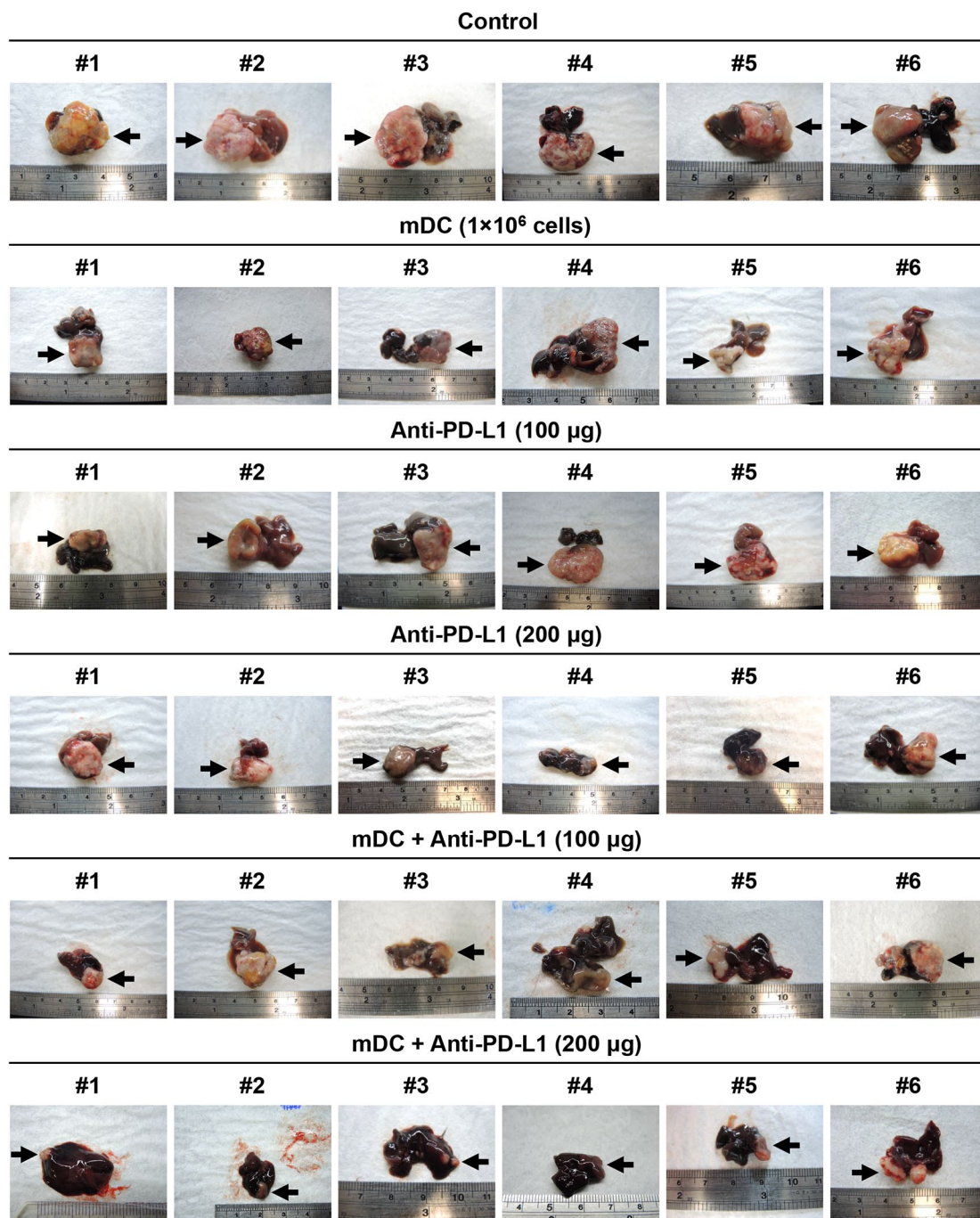
**Figure 6.** Examination of HCC tumor growth in the liver of each treatment group of mice. Tumor growth in the liver of the orthotopic HCC mice following treatment with the mDC ($1 \times 10^6$ cells/dose) and/or anti-PD-L1 (100 or 200 µg/dose). Six mice (denoted as #1 to #6) were used in each treatment group. The tumors are indicated with black arrows.
DC, dendritic cells; HCC, hepatocellular carcinoma; mDC, mature DC.

0.2–32.9), $P = 0.0038$ *versus* mDC ($1 \times 10^6$ cells/dose) and 0.0264 *versus* anti-PD-L1 (200 µg/dose)] (Figure 7). The significant difference in tumor volume between single and combination treatment was shown in the mDC combined with high dosage rather than low dosage of anti-PD-L1, suggesting that the mDC combined with anti-PD-L1 treatment decreased tumor volume
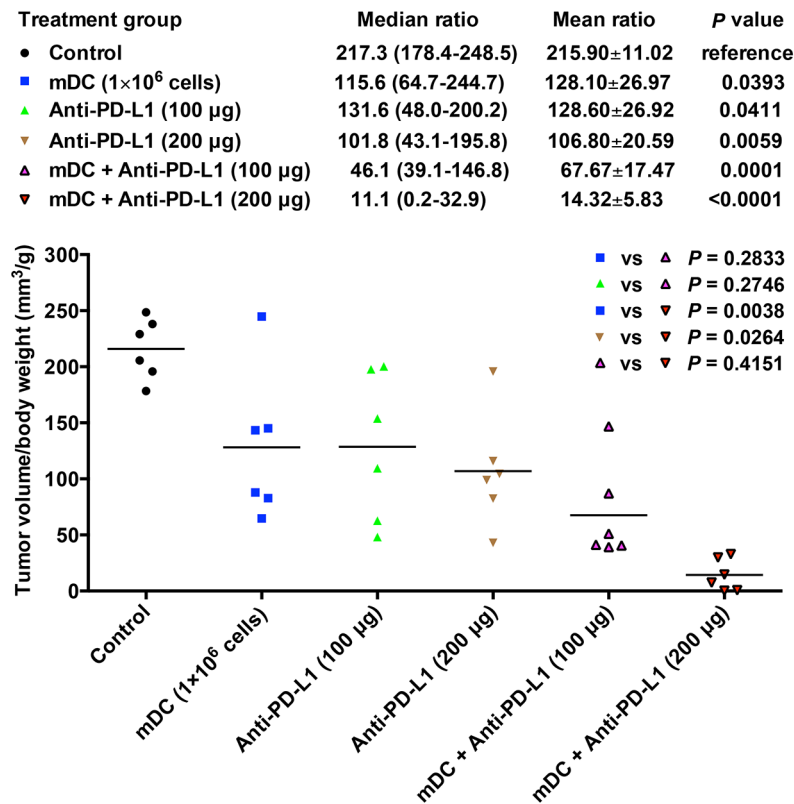
| Treatment group | Median ratio | Mean ratio | *P* value |
|---|---|---|---|
| ● Control | 217.3 (178.4-248.5) | 215.90±11.02 | reference |
| ■ mDC (1×10⁶ cells) | 115.6 (64.7-244.7) | 128.10±26.97 | 0.0393 |
| ▲ Anti-PD-L1 (100 µg) | 131.6 (48.0-200.2) | 128.60±26.92 | 0.0411 |
| ▼ Anti-PD-L1 (200 µg) | 101.8 (43.1-195.8) | 106.80±20.59 | 0.0059 |
| △ mDC + Anti-PD-L1 (100 µg) | 46.1 (39.1-146.8) | 67.67±17.47 | 0.0001 |
| ▽ mDC + Anti-PD-L1 (200 µg) | 11.1 (0.2-32.9) | 14.32±5.83 | <0.0001 |



**Figure 7.** Evaluation of HCC tumor volume in the liver of each treatment group of mice. Graph showing the ratio of tumor volume to body weight in the orthotopic HCC mice following treatment with the mDC ($1 \times 10^6$ cells/dose) and/or anti-PD-L1 (100 or 200 µg/dose). The horizontal lines represent the mean values. The tumor volume-to-body weight ratio in each group of mice ($n=6$) was shown as mean ± SEM and median (range). The significance of the difference of tumor volume-to-body weight ratio between different treatment groups of mice was analyzed and compared with the control group of mice. The significance of the difference of tumor volume-to-body weight ratio between single and combined treatment groups was also analyzed and is shown in the upper right corner of the graph. A *p* value $< 0.05$ was considered significant.
DC, dendritic cells; HCC, hepatocellular carcinoma; mDC, mature DC; vs, *versus*.

of mice in a dose-dependent manner; however, the difference between the mDC + anti-PD-L1 (100 µg/dose) and mDC + anti-PD-L1 (200 µg/dose) treatment did not reach statistical significance ($p=0.4151$). The tumor histopathology was also examined by H&E staining, though no obvious difference was found between different groups of mice (Figure S4).

*Combination treatment with the DC vaccine and PD-L1 inhibitor induced a higher level of tumor cell apoptosis than either treatment alone in the orthotopic HCC mice through triggering an increased infiltration of tumoricidal cytotoxic T cells*
To elucidate the therapeutic basis of the DC vaccine combined with PD-L1 inhibitor for HCC, the infiltration of DC and cytotoxic T cells in tumors of each treatment group of mice was

examined by fluorescent IHC staining. As shown in Figures S5, S6, S7, and S8, compared with the control group of mice, the levels of CD11c-positive and CD3/CD8 double-positive cells in tumor tissues were apparently higher in the groups of mice treated with the mDC either alone or combined with anti-PD-L1 than the other groups without mDC treatment [mean ± SEM (median, range); mDC ($1 \times 10^6$ cells/dose), $93.83 \pm 14.54$ cells/field (79.0, 64–149), $p < 0.0001$, $121.80 \pm 19.93$ cells/field (124.5, 38–180), $p < 0.0001$; anti-PD-L1 (100 µg/dose), $18.67 \pm 3.13$ cells/field (20.5, 9–28), $p=0.9474$, $10.67 \pm 1.92$ cells/field (9.5, 7–20), $p=0.9965$; anti-PD-L1 (200 µg/dose), $31.33 \pm 5.70$ cells/field (33.5, 10–47), $p=0.5339$, $12.00 \pm 2.19$ cells/field (11.5, 5–19), $p=0.9728$; mDC + anti-PD-L1 (100 µg/dose), $105.30 \pm 9.29$ cells/field (107.0, 78–131), $p < 0.0001$, $86.83 \pm 17.31$ cells/

field (73.0, 38 to 156), $p = 0.0069$; mDC + anti-PD-L1 (200 µg/dose), $130.70 \pm 18.92$ cells/field (124.0, 82 to 186), $p < 0.0001$, $108.50 \pm 22.34$ cells/field (119.0, 25–174), $p = 0.0004$, respectively], suggesting that administration of the DC vaccine could trigger an increased infiltration of tumor-specific DC and cytotoxic T cells. However, there was no obvious difference in DC and cytotoxic T cell infiltration between the mDC ($1 \times 10^6$ cells/dose), mDC + anti-PD-L1 (100 µg/dose), and mDC + anti-PD-L1 (200 µg/dose) groups.

Furthermore, the level of cell apoptosis in tumors of each treatment group of mice was also assessed by the TUNEL assay (Figure 8). As shown in Figure 8, the groups of mice treated with the mDC or anti-PD-L1 had a significantly increased number of apoptotic tumor cells compared with the control group of mice, though the anti-PD-L1 treatment showed statistical significance only at high dosage [mean $\pm$ SEM (median, range); mDC ($1 \times 10^6$ cells/dose), $30.67 \pm 2.51$ cells/field (31.5, 21 to 39), $p < 0.0001$; anti-PD-L1 (100 µg/dose), $14.67 \pm 1.11$ cells/field (14.5, 11–19), $p = 0.1817$; anti-PD-L1 (200 µg/dose), $37.33 \pm 2.72$ cells/field (38.5, 25–44), $p < 0.0001$]. A significant difference in tumor cell apoptosis was also observed between the mDC ($1 \times 10^6$ cells/dose) and anti-PD-L1 (100 µg/dose; $p = 0.0032$) as well as anti-PD-L1 (100 µg/dose) and anti-PD-L1 (200 µg/dose; $p < 0.0001$).

Moreover, combination treatment with the mDC and anti-PD-L1 could induce a prominently higher number of apoptotic tumor cells than either treatment alone [mean $\pm$ SEM (median, range); mDC + anti-PD-L1 (100 µg/dose), $33.83 \pm 3.21$ cells/field (32.5, 24–45), $p = 0.9613$ *versus* mDC ($1 \times 10^6$ cells/dose) and 0.0003 *versus* anti-PD-L1 (100 µg/dose); mDC + anti-PD-L1 (200 µg/dose), $61.17 \pm 4.07$ cells/field (11.1, 0.2–32.9), $p < 0.0001$ *versus* either mDC ($1 \times 10^6$ cells/dose) or anti-PD-L1 (200 µg/dose)] (Figure 9). The group of mice treated with mDC + anti-PD-L1 (200 µg/dose) exhibited a significantly higher level of tumor cell apoptosis than those treated with mDC + anti-PD-L1 (100 µg/dose; $p < 0.0001$), indicating that the mDC combined with anti-PD-L1 treatment induced tumor cell apoptosis in a dose-dependent manner.

Cytotoxic T cells have been shown to exert their anti-tumor activity through releasing granules containing cytotoxic molecules such as granzyme B.[33] To ascertain the function of cytotoxic T cells in DC vaccine combined with anti-PD-L1 treatment, we next detected the expression level of granzyme B in tumors of each treatment group of mice by fluorescent IHC staining. As shown in Figure S9 and S10, the groups of mice treated with the mDC or anti-PD-L1 displayed a considerably elevated level of granzyme B-positive cells in tumors compared with the control group of mice; however, the group treated with low-dosage anti-PD-L1 did not reach statistical significance [mean $\pm$ SEM (median, range); mDC ($1 \times 10^6$ cells/dose), $11.33 \pm 1.45$ cells/field (10.5, 8–18), $p = 0.0441$; anti-PD-L1 (100 µg/dose), $8.16 \pm 1.47$ cells/field (7.0, 5–15), $p = 0.3323$; anti-PD-L1 (200 µg/dose), $11.50 \pm 1.76$ cells/field (11.0, 7–17), $p = 0.0389$]. Remarkably, combination treatment with the mDC and anti-PD-L1 induced a significantly higher number of granzyme B-positive cells in tumors than either treatment alone in a dose-dependent manner [mean $\pm$ SEM (median, range); mDC + anti-PD-L1 (100 µg/dose), $21.17 \pm 1.24$ cells/field (21.0, 17–25), $P = 0.0343$ *versus* mDC ($1 \times 10^6$ cells/dose) and 0.0025 *versus* anti-PD-L1 (100 µg/dose); mDC + anti-PD-L1 (200 µg/dose), $36.00 \pm 4.38$ cells/field (33.5, 25–52), $p < 0.0001$ *versus* either mDC ($1 \times 10^6$ cells/dose) or anti-PD-L1 (200 µg/dose) and 0.0005 *versus* mDC + anti-PD-L1 (100 µg/dose)].

## Discussion

Although DC-based vaccine has been shown to have a favorable safety and considerable promise in treating HCC patients, the overall results of current DC vaccine clinical trials do not yet generate significant survival benefits.[13,14] Therefore, to develop new strategies to increase the effectiveness of DC vaccine-induced immune responses to HCC is particularly important. The blockade of PD-1/PD-L1 immune checkpoint pathway has been recently shown to enhance anti-tumor immune responses and emerged as a promising immunotherapy for HCC patients.[28–30] In this study, we for the first time, to the best of our knowledge, evaluated the therapeutic efficacy of DC vaccine combined with PD-L1 immune checkpoint inhibitor in an established orthotopic HCC mouse model. Our results suggested that combination treatment with DC vaccine and PD-L1 inhibitor might hold great potential as a novel strategy for HCC treatment.
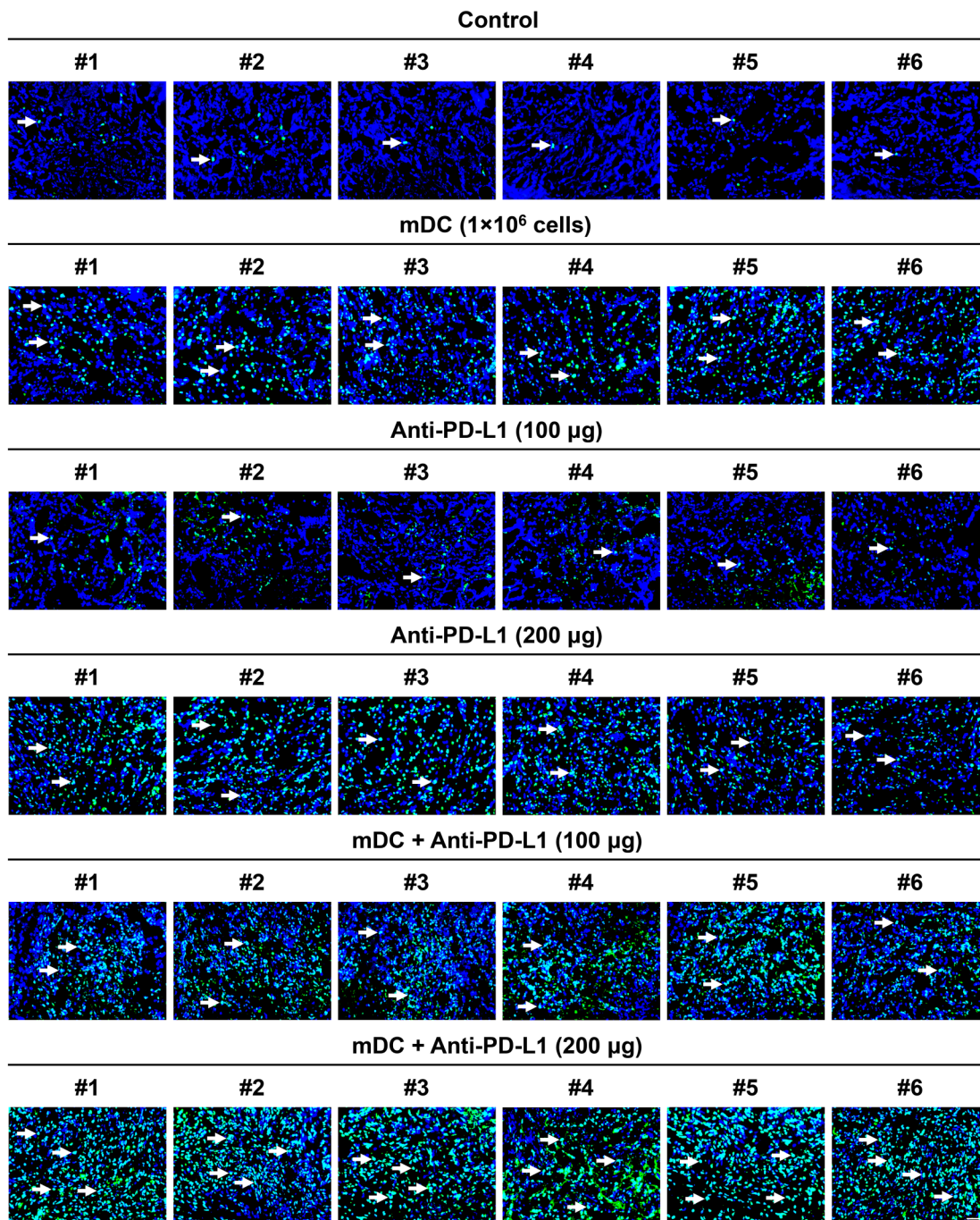
**Figure 8.** Assessment of cell apoptosis in tumors of each treatment group of mice. Apoptotic cells in tumors of the orthotopic HCC mice following treatment with the mDC ($1 \times 10^6$ cells/dose) and/or anti-PD-L1 (100 or 200 μg/dose) were visualized by TUNEL assay, as revealed by green nuclei. Counterstaining of apoptotic nuclei (green in color) with DAPI (blue in color) appeared cyan and is indicated by white arrows. Shown are representative results of six mice (denoted as #1 to #6) in each treatment group. Original magnification, ×63. Scale bar, 50 μm.
DAPI, 4′, 6-diamidino-2-phenylindole; DC, dendritic cells; HCC, hepatocellular carcinoma; mDC, mature DC; TUNEL, terminal deoxynucleotidyl transferase-mediated deoxyuridine triphosphate nick end-labeling.

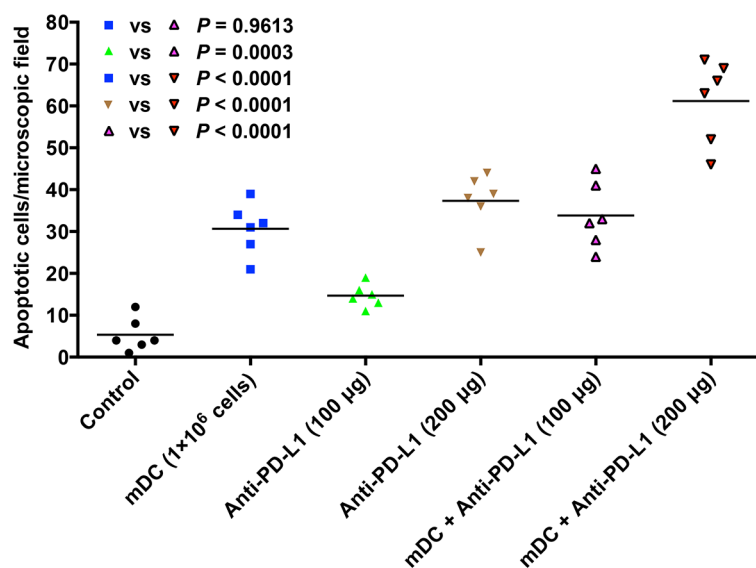| Treatment group | Median ratio | Mean ratio | P value |
|---|---|---|---|
| ● Control | 4.0 (1–12) | 5.33±1.62 | reference |
| ■ mDC (1×10⁶ cells) | 31.5 (21–39) | 30.67±2.51 | <0.0001 |
| ▲ Anti-PD-L1 (100 µg) | 14.5 (11–19) | 14.67±1.11 | 0.1817 |
| ▼ Anti-PD-L1 (200 µg) | 38.5 (25–44) | 37.33±2.72 | <0.0001 |
| ▲ mDC + Anti-PD-L1 (100 µg) | 32.5 (24–45) | 33.83±3.21 | <0.0001 |
| ▼ mDC + Anti-PD-L1 (200 µg) | 64.5 (46–71) | 61.17±4.07 | <0.0001 |



**Figure 9.** Quantitative evaluation of apoptotic cells in tumors of each treatment group of mice. Graph showing the number of apoptotic cells per microscopic field (original magnification, ×63) in tumor tissues of the orthotopic HCC mice following treatment with the mDC (1 × 10⁶ cells/dose) and/or anti-PD-L1 (100 or 200 µg/dose). The horizontal lines represent the mean values. The number of apoptotic cells per field in each group of mice ($n = 6$) is shown as mean ± SEM and median (range). The significance of the difference of apoptotic tumor cell number per field between different treatment groups of mice was analyzed and compared with the control group of mice. The significance of the difference of apoptotic tumor cell number per field between single and combined treatment groups was also analyzed and is shown in the upper left corner of the graph. A p value <0.05 was considered significant.
DC, dendritic cells; HCC, hepatocellular carcinoma; mDC, mature DC; vs, *versus*.

In this study, the C57BL/6J mouse strain was chosen because it is immune-competent and has a low frequency of spontaneous cancer. There are two reasons supporting that Hep-55.1C cells are better than another mouse hepatoma Hepa1.6 cells to be used in establishing the mouse model. First, Hep-55.1C cells are much more tumorigenic than Hepa1.6 cells.[31] Second, Hep-55.1C cells are derived from a C57BL/6J tumor and will not induce tumor rejection when injected into the C57BL/6J mouse strain.[34] Moreover, the mouse model established with Hep-55.1C cells has been well characterized to develop tumors resembling a poorly differentiated human HCC with a high level of cell proliferation, fibrosis, and steatosis, as well as an increased expression of several HCC markers.[31] Although, compared with the model of indirect portal vein injection, not all tumors display portal vein spread, lymph node, and distant metastasis, the model of direct injection of Hep-55.1C cells into the liver lobe has been shown to be the most appropriate for the rapid development of an orthotopic single tumor nodule in the liver with an incidence of 100%.[31] Therefore, we apply this model in this study to evaluate the efficacy of the DC vaccine combined with PD-L1 inhibitor in the treatment of primary HCC.

Two major sources of antigens have been employed to pulse DC for the preparation of antitumor DC vaccine, one being whole tumor cell lysates and the other being specific tumor antigen peptides.[15–18] Compared with the peptides derived from individual tumor antigens, whole tumor cell lysates contain a substantially larger number of

antigens, allowing for developing broadly applicable, as well as patient-specific, DC vaccines.[35] This property may be especially important in the development of the DC vaccine against HCC when considering the extremely high tumor heterogeneity and lack of main driver oncoproteins in HCC.[36,37] Therefore, in this study, we chose to use whole tumor cell lysates as antigens for pulsing DC in the generation of DC vaccine. Our data showed that the DC vaccine we prepared exhibited an appropriate morphology, high purity and maturity, and optimal maturation and functions. Treatment with the DC vaccine could significantly prolong overall survival and decrease tumor volume compared with untreated control in the orthotopic HCC mice.

It has been shown that the efficacy of the DC vaccine in cancer therapy is based on the activity of DC to induce T cell activation and proliferation, promote T cell infiltration into tumor, and trigger anti-tumor immune responses to destroy tumor cells. However, several immunosuppressive mechanisms have been shown to become activated within the tumor microenvironment of HCC, facilitating HCC cells to escape anti-tumor immune responses.[38–41] Among these mechanisms, the interaction between PD-1 and PD-L1 immune checkpoints plays a key role in preventing HCC cells from cytotoxic T cell attack.[22–24] Therefore, it is reasonable to speculate that the blockade of the PD-1/PD-L1 immune checkpoint pathway may have the potential to restore or enhance DC vaccine-induced anti-tumor immunity against HCC. In support of this notion, inhibition of PD-1/PD-L1 immune checkpoints during DC vaccination have been shown to exhibit better therapeutic effects than the DC vaccination alone in mouse models of breast cancer, melanoma, and glioblastoma.[42–45] Moreover, multiple clinical trials are currently in progress to evaluate the efficacy of the DC-based vaccine in combination with PD-1/PD-L1 immune checkpoint inhibitors in the treatment of various types of cancers, including melanoma, non-Hodgkin lymphoma, multiple myeloma, renal cell carcinoma, glioblastoma, non-small-cell lung cancer, and colorectal cancer.[46–48] However, to date, there is no literature that addresses the therapeutic efficacy of such combination treatment in HCC. In this study, we showed that treatment with antibody blocking PD-1/PD-L1 interactions, similar to DC vaccine, could significantly increase overall survival, decrease tumor volume, and induce tumor cell apoptosis compared with untreated control in the orthotopic HCC mice. Remarkably, combination treatment with DC vaccine and PD-L1 antibody could lead to considerably longer overall survival, smaller tumor volume, and higher tumor cell apoptosis than either treatment alone through inducing a stronger anti-tumor cytotoxic T cell response.

There are some limitations to this study. One limitation concerns the *in vivo* administration route of the DC vaccine and PD-L1 inhibitor. The DC vaccine and PD-L1 inhibitor were injected into mice subcutaneously and intraperitoneally, respectively. The efficacy of other routes of administration remains to be clarified. Another limitation is related to the treatment regimen. There was only one dosage of DC vaccine being administered to mice at 1-day intervals for three total doses. Whether treatment of a higher dosage of DC vaccine combined with PD-L1 inhibitor at higher total doses lead to a better efficacy remains to be evaluated. Furthermore, the number of mice used in each treatment group was somewhat small though statistical significance was reached. In addition, besides cytotoxic T cells, nature killer cells have been linked to the anti-tumor immune responses elicited by the DC vaccine,[49] and have been shown to contribute to cancer immunotherapy mediated by PD-1/PD-L1 blockade.[50] The role of nature killer cells in the therapeutic efficacy of DC vaccine combined with PD-L1 inhibitor in HCC remains to be elucidated. Even so, this study is the first study to our knowledge to provide proof of concept that the combination of DC vaccine and PD-L1 inhibitor shows therapeutic effect on HCC in an orthotopic mouse model.

In conclusion, the results of our study demonstrated that combination therapy with DC vaccination (induction of tumor-specific immunity) and PD-1/PD-L1 immune checkpoint blockade (enhancement of anti-tumor immunity) might represent a promising strategy for the treatment of HCC. Considering the encouraging results from other cancer types, further clinical trials are worth conducting to evaluate the efficacy of such combination therapy in HCC patients.

**ORCID iD**
Long-Bin Jeng [iD] https://orcid.org/0000-0002-4588-2268

**Supplemental material**
Supplemental material for this article is available online.

### References

1. Venook AP, Papandreou C, Furuse J, *et al*. The incidence and epidemiology of hepatocellular carcinoma: a global and regional perspective. *Oncologist* 2010; 15(Suppl. 4): 5–13.

2. Forner A, Llovet JM and Bruix J. Hepatocellular carcinoma. *Lancet* 2012; 379: 1245–1255.

3. Cheng KC, Lin WY, Liu CS, *et al*. Association of different types of liver disease with demographic and clinical factors. *Biomedicine (Taipei)* 2016; 6: 16.

4. Wall WJ and Marotta PJ. Surgery and transplantation for hepatocellular cancer. *Liver Transpl* 2000; 6: S16–S22.

5. Alsowmely AM and Hodgson HJ. Non-surgical treatment of hepatocellular carcinoma. *Aliment Pharmacol Ther* 2002; 16: 1–15.

6. Llovet JM and Bruix J. Novel advancements in the management of hepatocellular carcinoma in 2008. *J Hepatol* 2008; 48(Suppl. 1): S20–S37.

7. Marin-Hargreaves G, Azoulay D and Bismuth H. Hepatocellular carcinoma: surgical indications and results. *Crit Rev Oncol Hematol* 2003; 47: 13–27.

8. Llovet JM, Ricci S, Mazzaferro V, *et al*. Sorafenib in advanced hepatocellular carcinoma. *N Engl J Med* 2008; 359: 378–390.

9. Shaaban S, Negm A, Ibrahim EE, *et al*. Chemotherapeutic agents for the treatment of hepatocellular carcinoma: efficacy and mode of action. *Oncol Rev* 2014; 8: 246.

10. Steinman RM. The dendritic cell system and its role in immunogenicity. *Annu Rev Immunol* 1991; 9: 271–296.

11. Banchereau J and Steinman RM. Dendritic cells and the control of immunity. *Nature* 1998; 392: 245–252.

12. Banchereau J, Briere F, Caux C, *et al*. Immunobiology of dendritic cells. *Annu Rev Immunol* 2000; 18: 767–811.

13. Palucka K and Banchereau J. Cancer immunotherapy via dendritic cells. *Nat Rev Cancer* 2012; 12: 265–277.

14. Shang N, Figini M, Shangguan J, *et al*. Dendritic cells based immunotherapy. *Am J Cancer Res* 2017; 7: 2091–2102.

15. Lee WC, Wang HC, Hung CF, *et al*. Vaccination of advanced hepatocellular carcinoma patients with tumor lysate-pulsed dendritic cells: a clinical trial. *J Immunother* 2005; 28: 496–504.

16. Palmer DH, Midgley RS, Mirza N, *et al*. A phase II study of adoptive immunotherapy using dendritic cells pulsed with tumor lysate in patients with hepatocellular carcinoma. *Hepatology* 2009; 49: 124–132.

17. Butterfield LH, Ribas A, Potter DM, *et al*. Spontaneous and vaccine induced AFP-specific T cell phenotypes in subjects with AFP-positive hepatocellular cancer. *Cancer Immunol Immunother* 2007; 56: 1931–1943.

18. Sawada Y, Yoshikawa T, Nobuoka D, *et al*. Phase I trial of a glypican-3-derived peptide vaccine for advanced hepatocellular carcinoma: immunologic evidence and potential for improving overall survival. *Clin Cancer Res* 2012; 18: 3686–3696.

19. Kuol N, Stojanovska L, Nurgali K, *et al*. The mechanisms tumor cells utilize to evade the host's immune system. *Maturitas* 2017; 105: 8–15.

20. Roth GS and Decaens T. Liver immunotolerance and hepatocellular carcinoma: pathophysiological mechanisms and therapeutic perspectives. *Eur J Cancer* 2017; 87: 101–112.

21. Pardoll DM. The blockade of immune checkpoints in cancer immunotherapy. *Nat Rev Cancer* 2012; 12: 252–264.

22. Ishida Y, Agata Y, Shibahara K, *et al.* Induced expression of PD-1, a novel member of the immunoglobulin gene superfamily, upon programmed cell death. *EMBO J* 1992; 11: 3887–3895.

23. Freeman GJ, Long AJ, Iwai Y, *et al.* Engagement of the PD-1 immunoinhibitory receptor by a novel B7 family member leads to negative regulation of lymphocyte activation. *J Exp Med* 2000; 192: 1027–1034.

24. Iwai Y, Ishida M, Tanaka Y, *et al.* Involvement of PD-L1 on tumor cells in the escape from host immune system and tumor immunotherapy by PD-L1 blockade. *Proc Natl Acad Sci U S A* 2002; 99: 12293–12297.

25. Abdin SM, Zaher DM, Arafa EA, *et al.* Tackling cancer resistance by immunotherapy: updated clinical impact and safety of PD-1/PD-L1 inhibitors. *Cancers (Basel)* 2018; 10: 32.

26. Gong J, Chehrazi-Raffle A, Reddi S, *et al.* Development of PD-1 and PD-L1 inhibitors as a form of cancer immunotherapy: a comprehensive review of registration trials and future considerations. *J Immunother Cancer* 2018; 6: 8.

27. Hargadon KM, Johnson CE and Williams CJ. Immune checkpoint blockade therapy for cancer: An overview of FDA-approved immune checkpoint inhibitors. *Int Immunopharmacol* 2018; 62: 29–39.

28. Longo V, Gnoni A, Casadei Gardini A, *et al.* Immunotherapeutic approaches for hepatocellular carcinoma. *Oncotarget* 2017; 8: 33897–33910.

29. Kudo M. Immuno-oncology in hepatocellular carcinoma: 2017 update. *Oncology* 2017; 93(Suppl. 1): 147–159.

30. El-Khoueiry AB, Sangro B, Yau T, *et al.* Nivolumab in patients with advanced hepatocellular carcinoma (CheckMate 040): an open-label, non-comparative, phase 1/2 dose escalation and expansion trial. *Lancet* 2017; 389: 2492–2502.

31. Bour G, Martel F, Goffin L, *et al.* Design and development of a robotized system coupled to microCT imaging for intratumoral drug evaluation in a HCC mouse model. *PLoS One* 2014; 9: e106675.

32. Wu HC, Tsai HW, Teng CF, *et al.* Ground-glass hepatocytes co-expressing hepatitis B virus X protein and surface antigens exhibit enhanced oncogenic effects and tumorigenesis. *Hum Pathol* 2014; 45: 1294–1301.

33. Russell JH and Ley TJ. Lymphocyte-mediated cytotoxicity. *Annu Rev Immunol* 2002; 20: 323–370.

34. Kress S, Konig J, Schweizer J, *et al.* p53 mutations are absent from carcinogen-induced mouse liver tumors but occur in cell lines established from these tumors. *Mol Carcinog* 1992; 6: 148–158.

35. Chiang CL, Benencia F and Coukos G. Whole tumor antigen vaccines. *Semin Immunol* 2010; 22: 132–143.

36. Nault JC and Villanueva A. Intratumor molecular and phenotypic diversity in hepatocellular carcinoma. *Clin Cancer Res* 2015; 21: 1786–1788.

37. Lu LC, Hsu CH, Hsu C, *et al.* Tumor heterogeneity in hepatocellular carcinoma: facing the challenges. *Liver Cancer* 2016; 5: 128–138.

38. Fujiwara K, Higashi T, Nouso K, *et al.* Decreased expression of B7 costimulatory molecules and major histocompatibility complex class-I in human hepatocellular carcinoma. *J Gastroenterol Hepatol* 2004; 19: 1121–1127.

39. Arihara F, Mizukoshi E, Kitahara M, *et al.* Increase in CD14+HLA-DR -/low myeloid-derived suppressor cells in hepatocellular carcinoma patients and its impact on prognosis. *Cancer Immunol Immunother* 2013; 62: 1421–1430.

40. Chen KJ, Lin SZ, Zhou L, *et al.* Selective recruitment of regulatory T cell through CCR6-CCL20 in hepatocellular carcinoma fosters tumor progression and predicts poor prognosis. *PLoS One* 2011; 6: e24671.

41. Han Y, Chen Z, Yang Y, *et al.* Human CD14+ CTLA-4+ regulatory dendritic cells suppress T-cell response by cytotoxic T-lymphocyte antigen-4-dependent IL-10 and indoleamine-2,3-dioxygenase production in hepatocellular carcinoma. *Hepatology* 2014; 59: 567–579.

42. Ge Y, Xi H, Ju S, *et al.* Blockade of PD-1/PD-L1 immune checkpoint during DC vaccination induces potent protective immunity against breast cancer in hu-SCID mice. *Cancer Lett* 2013; 336: 253–259.

43. Nagaoka K, Hosoi A, Iino T, *et al.* Dendritic cell vaccine induces antigen-specific CD8+ T cells that are metabolically distinct from those of peptide vaccine and is well-combined with PD-1 checkpoint blockade. *Oncoimmunology* 2018; 7: e1395124.

44. Antonios JP, Soto H, Everson RG, *et al.* PD-1 blockade enhances the vaccination-induced immune response in glioma. *JCI Insight* 2016; 1: e87059.

45. Garzon-Muvdi T, Theodros D, Luksik AS, *et al*. Dendritic cell activation enhances anti-PD-1 mediated immunotherapy against glioblastoma. *Oncotarget* 2018; 9: 20681–20697.

46. Versteven M, Van den Bergh JMJ, Marcq E, *et al*. Dendritic cells and programmed death-1 blockade: a joint venture to combat cancer. *Front Immunol* 2018; 9: 394.

47. Saxena M and Bhardwaj N. Re-emergence of dendritic cell vaccines for cancer treatment. *Trends Cancer* 2018; 4: 119–137.

48. Bryant CE, Sutherland S, Kong B, *et al*. Dendritic cells as cancer therapeutics. *Semin Cell Dev Biol* 2018; 86: 77–88.

49. Karimi K, Boudreau JE, Fraser K, *et al*. Enhanced antitumor immunity elicited by dendritic cell vaccines is a result of their ability to engage both CTL and IFN gamma-producing NK cells. *Mol Ther* 2008; 16: 411–418.

50. Hsu J, Hodgins JJ, Marathe M, *et al*. Contribution of NK cells to immunotherapy mediated by PD-1/PD-L1 blockade. *J Clin Invest* 2018; 128: 4654–4668.